PHYSICAL REVIEW B **79**, 144104 (2009)

Local free energy in the paraelectric phase of barium titanate

Grégory Geneste*
Laboratoire Structures, Propriétés et Modélisation des Solides, CNRS-UMR 8580, Ecole Centrale Paris, Grande Voie des Vignes, 92295 Châtenay-Malabry Cedex, France
(Received 11 January 2009; published 3 April 2009)

A suitable definition for the local potential felt by local modes in the paraelectric phase of barium titanate is proposed. It is defined as the potential of mean force (free energy) acting on a given local mode $\vec{u}$. This free energy $\tilde{F}(\vec{u})$ is computed by constrained molecular dynamics coupled to the method of the thermodynamic integration. It is shown that this free-energy landscape is directly related to the density of probability of the local modes $\Pi(\vec{u})$ by $\Pi(\vec{u})=\Pi_0 e^{-[\tilde{F}(\vec{u})-\tilde{F}_0]/k_BT}$. From T_c to $\approx T_c+400$ K, the free-energy landscape obtained exhibits eight minima along the $\langle 111\rangle$ directions, confirming the existence of off-center dipoles in the paraelectric phase of barium titanate in this range of temperature. Only above this temperature, the free energy has a single minimum for $\vec{u}=\vec{0}$. An analytical expression of $\tilde{F}(\vec{u})$ is provided under the form of a fourth-order polynomial function in u_α.

DOI: 10.1103/PhysRevB.79.144104 PACS number(s): 64.60.Cn

I. INTRODUCTION

The high-temperature phase of ferroelectric crystals is of primary interest since the dynamics of the dipoles in this phase gives many indications about the deep nature (order-disorder versus displacive) of the ferroelectric-paraelectric phase transition and about the ferroelectricity itself. It has been very soon the subject of many theoretical[1–5] and experimental[6–8] studies and has been questioned more recently by modern simulation techniques.[9–12] In the case of barium titanate, the dynamics of the Ti ions inside their oxygen octahedron is indeed a crucial feature. The Ti motion has been related to the potential felt by these ions:[8] in the case of a purely displacive transition (associated to an underdamped soft mode), a harmonic potential well is expected whereas strong anharmonicities and a double-well profile (associated to an overdamped soft mode) are supposed to lead to an order-disorder transition.[8] Roughly speaking, the comparison of the depth of this potential well V_m with k_BT_c (T_c is the Curie temperature) is expected to allow a discrimination between these two limiting cases: $V_m \ll k_BT_c$ in the displacive case versus $V_m \gg k_BT_c$ in the order-disorder case.[8]

Since the strong development of first-principles calculations, much progress has been done in the understanding of the ferroelectric instability.[9] In particular, density-functional calculations have allowed an evaluation of the potential well in barium titanate at $T=0$ K: using, for example, the experimental cubic unit cell, the double well is found ≈ -30 meV per five-atom cell along the [111] direction[13] (and less deep along [110] and [100]). However, this value is obtained in the ferroelectric phase, i.e., in a microscopic configuration in which the atoms are displaced in the same way in all the unit cells. The energy profile is deduced from step by step computations in which the atoms are displaced along the soft mode. Thus, in the paraelectric phase, this "static" $T=0$ K potential is not suitable for understanding the dynamics of the system. In fact, it suffers from the lack of a clear definition in the high-temperature phase. The concept of *potential energy* can be used, indeed, only for an instantaneous description of the forces felt by the displacing atoms that strongly fluctuate with time. Intuitively, the introduction of an appropriate *thermodynamic potential* describing the local fluctuations of each dipole would be interesting for interpreting some properties of the high-temperature phase. Using such a thermodynamic potential, the displacive versus order-disorder character of a ferroelectric would be estimated by comparing k_BT_c and ΔF_m, the depth of the free-energy landscape just above T_c.

However, the simulation of the paraelectric phase is possible by using effective Hamiltonians, a powerful tool introduced by Zhong *et al.*[9,14] to describe the microscopic configurations of ferroelectric crystals through a reduction in the number of degrees of freedom. Roughly speaking, the effective Hamiltonians are simplifications of the microscopic energy landscape in terms of local modes $\vec{u}_i$ (i is the index of the unit cell) that represent the local polar displacements in each unit cell of the crystal, of displacement modes $\vec{v}_i$ (related to the inhomogeneous strain), and of homogeneous strain. Their parameters are fitted on first-principles calculations. For more complex perovskites, they can also include antiferrodistortive modes[15] or magnetic moments[16] (in the case of multiferroic crystals). Within this tool, the thermodynamics of ferroelectric materials can be reproduced by the standard atomic-scale simulation techniques such as Monte Carlo (MC) or molecular dynamics (MD).

In barium titanate, if the local modes are all frozen to zero, displacing one of them only (i.e., creating a single dipole in a nonpolar environment) is not enough to decrease the energy of the system.[17] In fact, in the paraelectric phase, at a given time t, the local modes are zero only on average and exhibit instantaneously a random pattern in which complex correlations do exist. Therefore, the force felt by a displacing local mode must be thought *on average*, and the relevant associated potential must be thought as that of the mean force felt by the displacing atoms, rather than that of the instantaneous force. In terms of mean force, we show hereafter that the related potential is in fact a *free energy* (thermodynamic potential).

The instantaneous and averaged potential felt by a given local mode in barium titanate has been nicely investigated in

the framework of the first-principles derived effective Hamiltonian of Zhong *et al.*[9] by Marqués[18] from Monte Carlo simulations. He showed that in the paraelectric phase of barium titanate, the instantaneous potential felt by a local mode on a given site exhibits a single minimum with position and depth changing in time. The deepest minima are found anyway at eight off-center regions located along the $\langle 111 \rangle$ directions. Averaging the instantaneous potentials leads to a potential with a single minimum located at the center of the unit cell (no polar displacement). In the present work, we propose to define a local thermodynamic potential which is different from the averaged potential calculated by Marqués.

The distribution of the local modes around the centers of the different unit cells can be related to the displacive or order-disorder character of the dynamics in the paraelectric phase. This distribution is controlled by the potential felt by the dipoles around their site. In the following, we will deal with the density of probability of the local modes, denoted as $\Pi(\vec{u})$. This quantity describes their distribution in the configuration space and is defined as follows: if the (equilibrated) system considered contains N unit cells (and thus N local modes), the number of local modes inside an infinitesimal volume $d\vec{u}$ around $\vec{u}$ at a given time t is $N\Pi(\vec{u})d\vec{u}$. Within this definition, this quantity is naturally normalized, $\int \Pi(\vec{u})d\vec{u}=1$.

In this work, we use the effective Hamiltonian of Zhong *et al.*,[9] coupled to molecular-dynamics simulations, to show that:

(i) $\Pi(\vec{u})$ is related to a *free-energy* landscape seen by the dipoles $\tilde{F}(\vec{u})$ through $\Pi(\vec{u})=\Pi_0 e^{-[\tilde{F}(\vec{u})-\tilde{F}_0]/k_BT}$,

(ii) this local free-energy landscape $\tilde{F}(\vec{u})-\tilde{F}_0$ is the potential of the mean force acting on a given local mode and can be computed by thermodynamic integration with constrained molecular dynamics, since its derivative $\frac{\partial \tilde{F}}{\partial \vec{u}}$ is minus the mean force felt by a given dipole,

(iii) this free-energy landscape $\tilde{F}(\vec{u})-\tilde{F}_0$ has eight minima located along the $\langle 111 \rangle$ directions up to very high temperatures ($\approx T_c+400$ K), and

(iv) $\tilde{F}(\vec{u})-\tilde{F}_0$ can be modeled very well under the form of a fourth-order polynomial function $a_1(u_x^2+u_y^2+u_z^2)+a_{11}(u_x^4+u_y^4+u_z^4)+a_{12}(u_x^2u_y^2+u_x^2u_z^2+u_y^2u_z^2)$. The coefficients a_1, a_{11}, and a_{12} are computed as a function of temperature (in the range of 300–700 K) and an analytical expression is proposed.

The calculation of a local free energy is directly inspired by the computation of incomplete free energies by thermodynamic integration methods as a function of an atom or molecule position in various kinds of systems (distance between a molecule and a surface[19] and adatom position on a surface[20] for example). It is well known that these incomplete free energies are directly related to the density of probability of this atom or molecule position. Following these ideas, we define in Sec. II an incomplete free energy $\tilde{F}(\vec{u})$ as a function of local mode $\vec{u}$ and show that it is directly related to the density of probability of the local modes. Rather than calculating it directly from the probability distribution of the dipoles, we use the thermodynamic integration method exactly as in the previously mentioned studies. In Sec. III the details of the molecular-dynamics study are presented. The results are given in Sec. IV. We show in particular that the free energy has eight minima along the [111] directions, corresponding to maxima of the density of probability, up to very high temperatures. The results are discussed in Sec. V.

II. THEORY

Let us begin by reminding some elementary definitions of statistical physics, adapted to the formalism of the effective Hamiltonian. In this framework, the degrees of freedom are the local modes $\vec{u}_i$ (i is the index of the unit cell) and the displacement modes (related to the inhomogeneous strain) $\vec{v}_i$. We consider a system with N unit cells.

The microscopic states of the system are all the $\{\vec{u}_1 \ldots \vec{u}_N, \vec{p}_1 \ldots \vec{p}_N, \vec{v}_1 \ldots \vec{v}_N, \vec{p}'_1 \ldots \vec{p}'_N\}$, in which $\vec{p}_i$ ($\vec{p}'_i$) are the conjugate momenta of $\vec{u}_i$ ($\vec{v}_i$). In the following, for convenience, we omit the displacement modes $\vec{v}_i$ and their conjugate momenta $\vec{p}'_i$ (it would be very easy to add them to the following definitions, without changing the final formulas).

The energy of a microscopic state $\{\vec{u}_1 \ldots \vec{u}_N, \vec{p}_1 \ldots \vec{p}_N\}$ is

$$E(\{\vec{u}_1 \ldots \vec{u}_N, \vec{p}_1 \ldots \vec{p}_N\}) = \sum_{i=1}^{N} \frac{\vec{p}_i^2}{2m_{lm}} + H^{\text{eff}}(\vec{u}_1 \ldots \vec{u}_N)$$

with H^{eff} being the effective Hamiltonian and m_{lm} being the mass associated to the local modes. In this framework, the canonical partition function writes

$$Z = \frac{1}{h^{3N}} \int d\vec{p}_i \int d\vec{u}_i \, e^{-\beta E(\vec{u}_1 \ldots \vec{u}_N, \vec{p}_1 \ldots \vec{p}_N)} \tag{1}$$

with $\beta=1/k_BT$. The notation $\int d\vec{u}_i$ stands for the $3N$-dimensional integral $\int \cdots \int d\vec{u}_1 \ldots d\vec{u}_N$ (idem for $\int d\vec{p}_i$). In this expression, $1/N!$ is omitted since the local modes are discernable (they are attached to well-identified unit cells).

The density of probability of the microscopic state $\{\vec{u}_1 \ldots \vec{u}_N, \vec{p}_1 \ldots \vec{p}_N\}$ is

$$P(\vec{u}_1 \ldots \vec{u}_N, \vec{p}_1 \ldots \vec{p}_N) = \frac{e^{-\beta E(\vec{u}_1 \ldots \vec{u}_N, \vec{p}_1 \ldots \vec{p}_N)}}{h^{3N} Z}. \tag{2}$$

This means that the (dimensionless) probability for the system to be found in the infinitesimal volume $\delta^3\vec{u}_1 \cdots \delta^3\vec{u}_N \delta^3\vec{p}_1 \cdots \delta^3\vec{p}_N$ around the microscopic state $\{\vec{u}_1 \ldots \vec{u}_N, \vec{p}_1 \ldots \vec{p}_N\}$ is

$$\delta P = \frac{e^{-\beta E(\vec{u}_1 \ldots \vec{u}_N, \vec{p}_1 \ldots \vec{p}_N)}}{h^{3N} Z} \delta^3\vec{u}_1 \cdots \delta^3\vec{u}_N \delta^3\vec{p}_1 \cdots \delta^3\vec{p}_N. \tag{3}$$

The ensemble average of the microscopic quantity $A(\vec{u}_1 \ldots \vec{u}_N, \vec{p}_1 \ldots \vec{p}_N)$ is

$$\langle A \rangle = \frac{1}{h^{3N}} \int d\vec{p}_i \int d\vec{u}_i \, A(\vec{u}_1 \ldots \vec{u}_N, \vec{p}_1 \ldots \vec{p}_N) \frac{e^{-\beta E(\vec{u}_1 \ldots \vec{u}_N, \vec{p}_1 \ldots \vec{p}_N)}}{Z}.$$

A. Incomplete partition function

We now focus on one particular unit cell (the number one for instance $i=1$) and redefine all these quantities for a fixed

value of the local mode $\vec{u}_1$ attached to this unit cell. First, we define an incomplete partition function $\tilde{Z}^{(1)}(\vec{u})$ for $\vec{u}_1=\vec{u}$ by

$$\tilde{Z}^{(1)}(\vec{u}) = \frac{a_0^3}{h^{3N}} \int d\vec{p}_i \int d\vec{u}_i \; \delta(\vec{u}_1 - \vec{u}) e^{-\beta E(\vec{u}_1 \ldots \vec{u}_N, \vec{p}_1 \ldots \vec{p}_N)},$$

which simplifies to

$$\tilde{Z}^{(1)}(\vec{u}) = \frac{a_0^3}{h^{3N}} \int d\vec{p}_i \int d\vec{u}_2 \ldots d\vec{u}_N e^{-\beta E(\vec{u}_1 = \vec{u}, \ldots \vec{u}_N, \vec{p}_1 \ldots \vec{p}_N)}. \quad (4)$$

The superscript (1) means that the incomplete partition function is constructed by fixing the value of the local mode in the cell $i=1$. The summation is extended over all the microscopic states with $\vec{u}_1=\vec{u}$. a_0 is the lattice constant of cubic barium titanate. With such a definition, the incomplete partition function is dimensionless and we have

$$Z = \int_{\vec{e}_1} \tilde{Z}^{(1)}(\vec{u}_1) d\vec{e}_1 \quad (\vec{u}_1 = a_0 \vec{e}_1). \quad (5)$$

Note that the constant a_0^3 is introduced to make the partition function dimensionless but it has not a real importance: a multiplicative constant in the partition function $\tilde{Z}$ induces an additive constant in the free energy, and we will show hereafter that only differences of free energy are important for us.

Moreover, the simulated system is homogeneous; thus, it is obvious that the definition of $\tilde{Z}(\vec{u})$ does not depend on the selected unit cell ($i=1$): one would obtain the same function with any value of i: $\tilde{Z}^{(1)}(\vec{u})=\tilde{Z}^{(2)}(\vec{u})=\cdots=\tilde{Z}^{(N)}(\vec{u})$. The superscript (1) is thus now omitted in what follows and $\tilde{Z}(\vec{u})$ is *a priori* well defined.

On the other hand, the density of probability for the local mode $\vec{u}_1$ to be equal to $\vec{u}$ is obtained by summing the probabilities of all the microscopic states corresponding to the fixed value of $\vec{u}_1=\vec{u}$,

$$\Pi(\vec{u}) = \int d\vec{p}_i \int d\vec{u}_2 \ldots d\vec{u}_N P(\vec{u}_1 = \vec{u}, \ldots \vec{u}_N, \vec{p}_1 \ldots \vec{p}_N). \quad (6)$$

It also writes

$$\Pi(\vec{u}) = \int d\vec{p}_i \int d\vec{u}_1 \ldots d\vec{u}_N \delta(\vec{u}_1 - \vec{u}) \frac{e^{-\beta E(\vec{u}_1 \ldots \vec{u}_N, \vec{p}_1 \ldots \vec{p}_N)}}{h^{3N} Z}.$$

One can check easily that this density of probability is normalized,

$$\int_{\vec{u}} \Pi(\vec{u}) d\vec{u} = 1, \quad (7)$$

and corresponds to the definition given in Sec. I.

There is a simple relation between $\Pi(\vec{u})$ and $\tilde{Z}(\vec{u})$,

$$a_0^3 Z \Pi(\vec{u}) = \tilde{Z}(\vec{u}). \quad (8)$$

The ensemble average of the microscopic quantity $A(\vec{u}_1 \ldots \vec{u}_N, \vec{p}_1 \ldots \vec{p}_N)$ under the constraint $\vec{u}_1=\vec{u}$ is

$$\langle A \rangle(\vec{u}) = \frac{a_0^3}{h^{3N}} \int d\vec{p}_i \int d\vec{u}_i \delta(\vec{u}_1 - \vec{u}) A(\vec{u}_1 \ldots \vec{u}_N, \vec{p}_1 \ldots \vec{p}_N) \times \frac{e^{-\beta E(\vec{u}_1 \ldots \vec{u}_N, \vec{p}_1 \ldots \vec{p}_N)}}{\tilde{Z}(\vec{u})}.$$

B. Incomplete free energy

We now define an incomplete free energy from the incomplete partition function as follows:

$$\tilde{F}(\vec{u}) = -k_B T \ln \tilde{Z}(\vec{u}). \quad (9)$$

From Eq. (8), the density of probability of the dipoles is thus directly related to $\tilde{F}$ by

$$\Pi(\vec{u}) = \frac{1}{a_0^3 Z} e^{-\tilde{F}(\vec{u})/k_B T}. \quad (10)$$

We define $\Pi_0=\Pi(\vec{u}=\vec{0})$,

$$\Pi_0 = \frac{1}{a_0^3 Z} e^{-\tilde{F}_0/k_B T}, \quad \tilde{F}_0 = \tilde{F}(\vec{u}=\vec{0}).$$

It follows that

$$\Pi(\vec{u}) = \Pi_0 e^{-[\tilde{F}(\vec{u}) - \tilde{F}_0]/k_B T}. \quad (11)$$

The normalization constant Π_0 can be obtained by Eq. (7).

C. Computation of $\tilde{F}(\vec{u})-\tilde{F}_0$

This local free energy could be *a priori* calculated directly from the density of probability of the local modes. Anyway, this method does not ensure that the high free-energy regions (which have a low probability to be explored) would be correctly sampled by the standard simulation techniques.

Instead we propose a more general method, which has been already successfully used in other systems.[19,20] It is based on the thermodynamic integration: the free energy is a quantity that cannot be computed by the standard simulation techniques (Monte Carlo or molecular dynamics) as the ensemble average of some microscopic quantity. Usually, only derivatives of the free energy are accessible from these techniques. In the case where only a difference of free energy between two states is desired (this is the case here), the knowledge of the derivative over a path joining these two states is enough to determine by integration this difference. This technique is called thermodynamic integration.[21]

In our case, we can write

$$\tilde{F}(\vec{u}) - \tilde{F}_0 = \oint \frac{\partial \tilde{F}}{\partial \vec{u}}(\vec{u}') \cdot d\vec{u}', \quad (12)$$

in which the integration is performed over a continuous path from $\vec{0}$ to $\vec{u}$ in the tridimensional space (u_x, u_y, u_z). We have thus to calculate $\frac{\partial \tilde{F}}{\partial \vec{u}}$. From Eq. (9), this quantity is

$$\frac{\partial \tilde{F}}{\partial \vec{u}} = -\frac{k_B T}{\tilde{Z}} \frac{\partial \tilde{Z}}{\partial \vec{u}}. \quad (13)$$

From the definition of $\tilde{Z}(\vec{u})$ [Eq. (4)], we have

$$\frac{\partial \tilde{Z}}{\partial \vec{u}} = -\frac{1}{k_B T}\frac{a_0^3}{h^{3N}}\int d\vec{p}_i \int d\vec{u}_2 \ldots d\vec{u}_N \frac{\partial H^{eff}}{\partial \vec{u}_1} e^{-\beta E(\vec{u}_1=\vec{u},\ldots\vec{u}_N,\vec{p}_1\ldots\vec{p}_N)}$$

and thus, since $\partial H^{\text{eff}}/\partial \vec{u}_1$ is minus the force acting on the $i=1$ local mode ($\vec{f}_1$),

$$\frac{\partial \tilde{F}}{\partial \vec{u}} = -\frac{k_B T}{\tilde{Z}}\frac{\partial \tilde{Z}}{\partial \vec{u}} = \frac{a_0^3}{h^{3N}}\int d\vec{p}_i \int d\vec{u}_1 \ldots d\vec{u}_N \delta(\vec{u}_1 - \vec{u}) \times\{-\vec{f}_1\}\frac{e^{-\beta E(\vec{u}_1\ldots\vec{u}_N,\vec{p}_1\ldots\vec{p}_N)}}{\tilde{Z}(\vec{u})},$$

in which we can recognize the thermal average under fixed $\vec{u}_1$ of the microscopic quantity $-\vec{f}_1$. The derivative of $\tilde{F}$ with respect to $\vec{u}$ is thus minus the thermal average (under fixed $\vec{u}_1$) of the force acting on the local mode $\vec{u}_1$,

$$\frac{\partial \tilde{F}}{\partial \vec{u}} = -\langle \vec{f}_1 \rangle_{\vec{u}_1=\vec{u}}. \tag{14}$$

The difference $\Delta\tilde{F}(\vec{u})=\tilde{F}(\vec{u})-\tilde{F}_0$ is obtained by integration,

$$\Delta\tilde{F}(\vec{u}) = \tilde{F}(\vec{u}) - \tilde{F}_0 = -\oint \langle \vec{f}_1 \rangle_{\vec{u}_1=\vec{u}'} \cdot d\vec{u}', \tag{15}$$

in which the integration is performed over any continuous path joining $\vec{u}=\vec{0}$ to $\vec{u}$ in the three-dimensional (3D) space (u_x,u_y,u_z). $\tilde{F}(\vec{u})$ is the potential of mean force (PMF) acting on a given local mode. The derivative of $\tilde{F}(\vec{u})$ with respect to $\vec{u}$ (i.e., its gradient) can thus be obtained, from a computational point of view, through simulations under constraint ($\vec{u}_1=\vec{u}$) and the free energy itself recovered after that by thermodynamic integration.

III. COMPUTATIONAL DETAILS

We perform MD simulations in the framework of the effective Hamiltonian developed by Zhong *et al.*[9,14] The method has been previously carefully tested on barium titanate:[22] it reproduces very well the temperature evolution of strain and polarization and the sequence of phase transitions, as expected from Monte Carlo simulations. In particular, the bulk properties of $BaTiO_3$ (BTO) are simulated using the Nosé-Hoover method to fix the temperature and the Parrinello-Rahman algorithm[23] to fix the pressure or stress.[22] In the present work, we use a $12\times12\times12$ supercell with periodic boundary conditions and a Nosé-Hoover[24–26] thermostat to fix the temperature. The forces on the local modes and displacement modes are obtained as minus the derivatives of the effective Hamiltonian with respect to the various degrees of freedom. These forces are included in Newton equations of motions for $\vec{u}_i$ and $\vec{v}_i$, which are integrated within the well-known Verlet algorithm.

For each temperature, we calculate the gradient of $\tilde{F}(\vec{u})$ along three directions, at points distant from each other by 0.001 a_0 (along each coordinate). As shown hereafter, the grid defined that way is fine enough to perform a correct integration. For a given value of $\vec{u}$, we perform 10^5 steps of constrained MD. This constrained MD consists in maintaining invariant the local mode $\vec{u}_1$ ($=\vec{u}$). The dynamics of all the other degrees of freedom is not changed. To maintain the constraint $\vec{u}_1=\vec{u}$, an additional ("external") force is added in the equation of motion of $\vec{u}_1$, precisely equal to $-\vec{f}_1$ at each step, so that

$$m_{lm}\frac{d^2\vec{u}_1}{dt^2} = \vec{0}. \tag{16}$$

By imposing the initial velocity of $\vec{u}_1$ to zero and the initial value of $\vec{u}_1$ to the desired value $\vec{u}$, the constraint $\vec{u}_1=\vec{u}$ is ensured all along the simulation. Note that this modified equation of motion can be obtained properly from the Lagrangian formalism. Let us call L the Lagrangian of the unconstrained system and L' that of the constrained one,

$$L' = L - \sum_\alpha \lambda_\alpha (u_{1,\alpha} - u_\alpha), \tag{17}$$

in which the λ_α are Lagrange multipliers and $u_{1,\alpha}$ and u_α the α components of $\vec{u}_1$ and $\vec{u}$. The Lagrange equations for the components of $\vec{u}_1$ are

$$m_{lm}\frac{d^2u_{1,\alpha}}{dt^2} = f_{1,\alpha} - \lambda_\alpha. \tag{18}$$

Imposing $u_{1,\alpha}$ invariant leads immediately to $\lambda_\alpha=f_{1,\alpha}$. The equations of motion of the other local modes are not modified,

$$\forall i \neq 1, \forall \alpha, m_{lm}\frac{d^2u_{i,\alpha}}{dt^2} = -\frac{\partial H^{\text{eff}}}{\partial u_{i,\alpha}} = f_{i,\alpha}. \tag{19}$$

For each run, the 50 000 first steps are used to equilibrate the system and the thermal average of $-\vec{f}_1$ is computed over the 50 000 last ones. The strain tensor is maintained fixed for all the temperatures. This is justified by the fact that with this effective Hamiltonian, there is no thermal expansion in the material. We fix $\eta_1=\eta_2=\eta_3=0.0121$ (and $\eta_4=\eta_5=\eta_6=0$). This strain corresponds, in the cubic phase, to an isotropic stress tensor corresponding to a negative pressure of −4.8 GPa (This is the pressure used by Zhong *et al.*[9] to correct the underestimation of the lattice constant within the local-density approximation).

Following Refs. 22 and 27, the mass associated to the local modes is 39.0 amu. All the calculations of the present paper are performed in the NVT ensemble (with Nosé-Hoover thermostat), except those of Secs. IV C and IV D which are performed in the NVE (microcanonical) ensemble.

The thermodynamic integration is performed through a finite-difference method: $\partial\tilde{F}/\partial u_\alpha$ is computed on a grid with points distant, along each direction, from $\Delta u=0.001a_0$. For example, the free energy along [100], thus at point $u_x=n.\Delta u$, $u_y=u_z=0$, is calculated by

$$\tilde{F}(u_x=n\Delta u, u_y=u_z=0) - \tilde{F}_0 = \Delta u\sum_{k=1}^{n}\left[\frac{\partial\tilde{F}}{\partial u_x}\right]_{k\Delta u}.$$

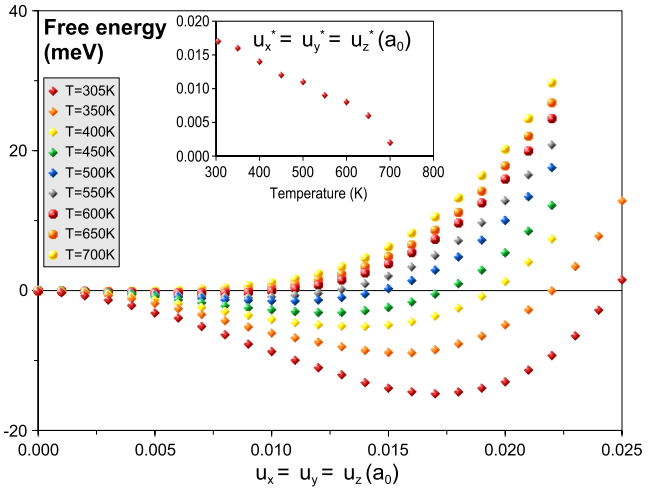

FIG. 1. (Color online) $\tilde{F}(\vec{u})-\tilde{F}_0$ (meV) along the [111] direction. Inset: temperature evolution of the components of the minimum of $\tilde{F}(\vec{u})$. The local mode is in a_0 units (a_0 is the lattice constant). $T_c \approx 300$ K with the present Hamiltonian.

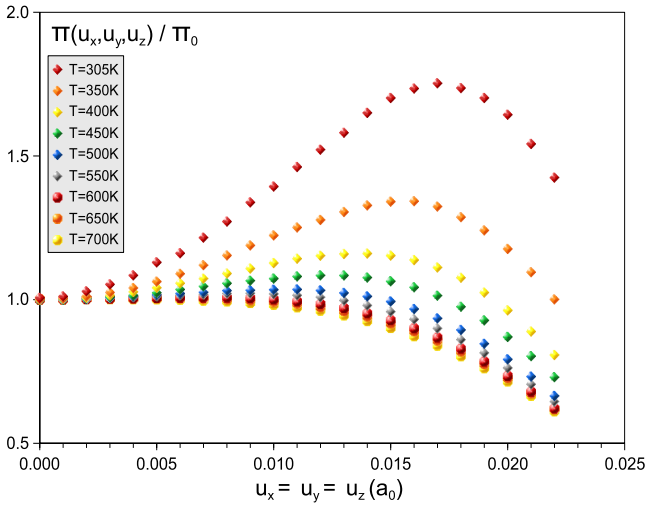

FIG. 2. (Color online) Density of probability $\Pi(\vec{u})$ (divided by Π_0) along the [111] direction. The local mode is in a_0 units (a_0 is the lattice constant). $T_c \approx 300$ K with the present Hamiltonian.

As a result, the numerical error related to the finite-difference scheme propagates linearly with the local mode $\vec{u}$. The maximal error along a given path, integrated from $\vec{u}=\vec{0}$ can be computed from the maximum of the second derivatives of the free energy. If we take as example the [111] direction just above T_c, the error at $u_x=u_y=u_z=0.020a_0$ can be estimated at ≈ 2 meV (0.1 meV per $0.001a_0$ along the path), which can be considered as small enough. Moreover, the numerical uncertainty on the position of the minima of the free energy is simply Δu. Systematic improvement is possible by using other finite-difference integration schemes (Simpson method for instance).

IV. RESULTS

A. Computation of $\tilde{F}(\vec{u})-\tilde{F}_0$ along the ⟨111⟩, ⟨110⟩, and ⟨100⟩ directions

The effective Hamiltonian of Zhong *et al.*[9,14] provides a Curie temperature of around 300 K.[9,14,28,29] Although this temperature is much lower than the true one, it has been shown that this Hamiltonian describes very well the sequence of phase transitions and temperature evolution of strain and polarization of barium titanate. Since we are interested in the high-temperature phase of BTO, we perform the MD simulations at $T=305$, 350, 400, 450, 500, 550, 600, 650, and 700 K.

The evolution of $\tilde{F}(\vec{u})-\tilde{F}_0$ as a function of $\vec{u}$ along the [111] direction is shown on Fig. 1. Just above T_c, the free-energy depth is ≈ -15 meV. These curves have a well pronounced minimum for $\vec{u}\neq\vec{0}$ up to ≈ 700 K (i.e., $\approx T_c$ +400 K in the framework of the effective Hamiltonian used). Above this temperature, the free energy along [111] has only one minimum for $u_x=u_y=u_z=0$. The temperature evolution of the components of the minimum of $\tilde{F}(\vec{u})$ (denoted as u_x^*, u_y^*, and u_z^*) is shown in the inset of Fig. 1. Since the ⟨111⟩ directions are all equivalent in the cubic phase of barium titanate, we have eight similar profiles along these lines.

The corresponding density of probability $\Pi(\vec{u})$, calculated from Eq. (11), is shown on Fig. 2 along the [111] direction. As expected, it presents a maximum for $\vec{u}\neq\vec{0}$ where the free energy has its minimum.

The free-energy profiles and corresponding densities of probability along [100] and [110] are shown on Figs. 3 and 4. The same tendencies are observed, but these curves are less deep than along [111] (a comparison is given for $T=305$ K in Fig. 5). The densities of probability also have a maximum for $\vec{u}\neq\vec{0}$ along these directions up to high temperatures. This maximum is located at the minimum of the free energy.

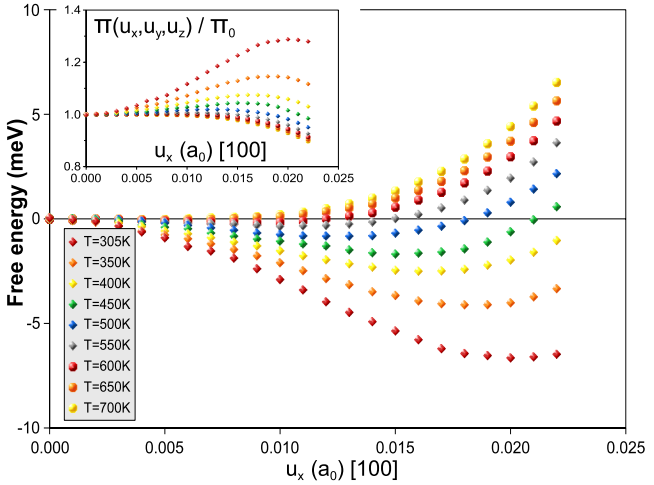

FIG. 3. (Color online) $\tilde{F}(\vec{u})-\tilde{F}_0$ (meV) along the [100] direction. Inset: density of probability $\Pi(\vec{u})$ (divided by Π_0) along the [100] direction, calculated from Eq. (11). The local mode is in a_0 units (a_0 is the lattice constant). $T_c \approx 300$ K with the present Hamiltonian.

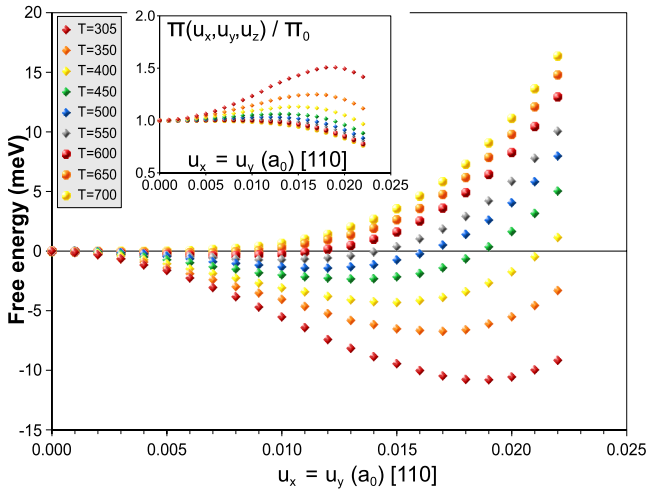

FIG. 4. (Color online) $\tilde{F}(\vec{u})-\tilde{F}_0$ (meV) along the [110] direction. Inset: density of probability $\Pi(\vec{u})$ (divided by Π_0) along the [110] direction, calculated from Eq. (11). The local mode is in a_0 units (a_0 is the lattice constant). $T_c \approx 300$ K with the present Hamiltonian.

B. Simple model for the local free energy

If seems natural to fit $\tilde{F}(\vec{u})-\tilde{F}_0$ by a polynomial function up to fourth order in u_x, u_y, and u_z [indeed, the minimum of $\tilde{F}(\vec{u})$ decreases continuously to zero, as the order parameter in a second-order phase transition[30]],

$$\begin{aligned}\tilde{F}(\vec{u}) - \tilde{F}_0 &= \Delta\tilde{F}(\vec{u}) \\ &= a_1(u_x^2+u_y^2+u_z^2) + a_{11}(u_x^4+u_y^4+u_z^4) \\ &\quad + a_{12}(u_x^2u_y^2+u_x^2u_z^2+u_y^2u_z^2).\end{aligned}$$

One expects a strong temperature variation of the quadratic coefficient a_1 that should vanish for $T=T_0\approx 700$ K according to our computations.

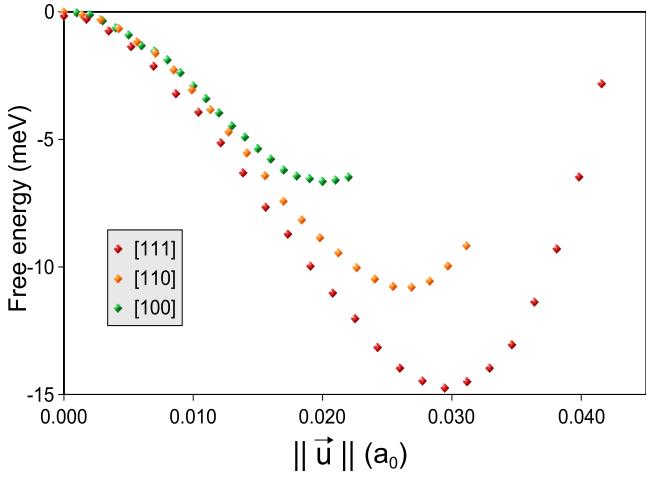

FIG. 5. (Color online) Local free energy (meV) at $T=305$ K as a function of $\|\vec{u}\|$ (in lattice constant units) along the [111], [110], and [100] directions. Note that the free energy is computed as a function of the norm of the local mode, rather than as a function of one component as in the other figures. $T_c \approx 300$ K with the present Hamiltonian.

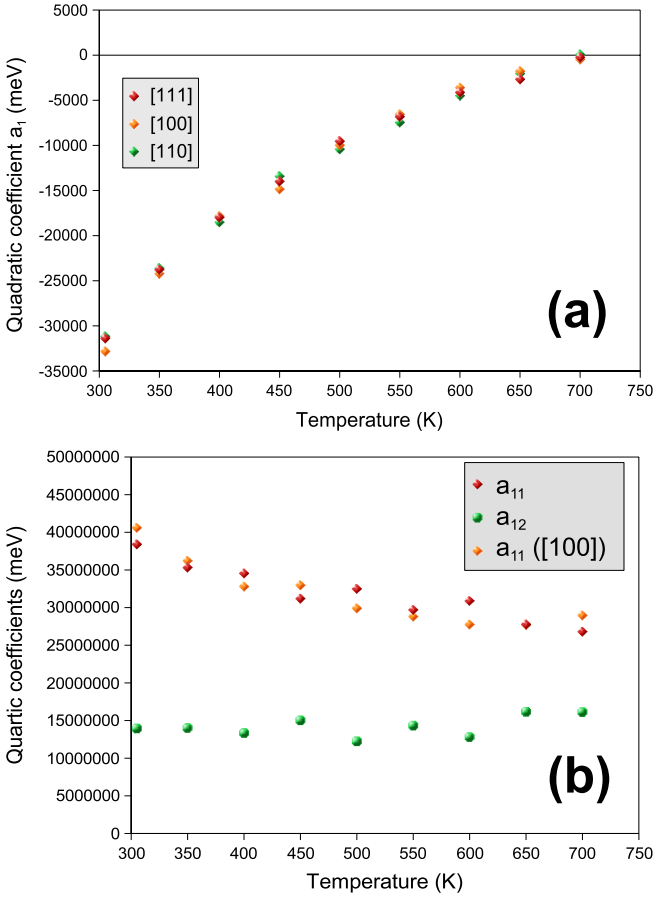

FIG. 6. (Color online) Temperature evolution of the quadratic and quartic coefficients a_1, a_{11}, and a_{12} (meV). (a) Quadratic coefficient a_1 as obtained from the free-energy profiles computed along [111] (red diamonds), [100] (orange diamonds), and [110] (green diamonds). (b) Quartic coefficients. Red diamonds: a_{11} as obtained from the computation of the free energy along [111] and [110]. Green circles: a_{12} as obtained from the computation of the free energy along [111] and [110]. Orange circles: a_{11} as obtained from the computation of the free energy along [100].

Along the [111] direction, this expression reduces to

$$\Delta\tilde{F}_{[111]}(\vec{u}) = 3a_1u_x^2 + 3(a_{11}+a_{12})u_x^4 \tag{20}$$

with $u_x=u_y=u_z$. Along the [100] direction, it reduces to

$$\Delta\tilde{F}_{[100]}(\vec{u}) = a_1u_x^2 + a_{11}u_x^4 \tag{21}$$

with $u_y=u_z=0$. Along the [110] direction, it reduces to

$$\Delta\tilde{F}_{[110]}(\vec{u}) = 2a_1u_x^2 + (2a_{11}+a_{12})u_x^4 \tag{22}$$

with $u_x=u_y$ and $u_z=0$.

First, the curves obtained fit very well by fourth-order polynomial functions without odd term. The temperature evolution of the coefficients is plotted on Fig. 6. We propose an analytical expression for these coefficients, under the form of a third order polynomial function in T for a_1, a constant for a_{12}, and a linear evolution for a_{11} (Table I). The

TABLE I. Analytical expressions for the temperature evolution of the coefficients of the free energy, relevant between 300 and 700 K. a_1, a_{11}, and a_{12} are in meV (they apply with local modes in a_0 units).

$$a_1 = 0.000366(T-T_0)^3 + 0.062(T-T_0)^2 + 46(T-T_0)$$
$$T_0 = 701 \text{ K}$$
$$a_{11} = -27500T + 45.582 \times 10^6$$
$$a_{12} = 14.2261 \times 10^6$$

given expressions are of course relevant in the range of 300–700 K. The coefficients are calculated in meV (they apply in the previous expressions with the local modes in a_0 units).

C. Example of local mode dynamics from direct molecular dynamics

The dynamics of a given local mode can be examined from direct molecular-dynamics simulations. We select in our $12 \times 12 \times 12$ supercell one site and plot the time evolution of one component of the corresponding local mode (Fig. 7). A relevant time evolution can *a priori* be obtained only in the NVE ensemble; thus, we flip to this numerical scheme.

It can be viewed that just above the Curie temperature, the selected component often flips from a direction to the other. It mostly oscillates either around a negative value or a positive one, confirming that there exists a free energy well at a nonzero value. Many recrossing phenomena can be observed.

As already said, each local mode $\vec{u}$ feels a free-energy landscape $\tilde{F}(\vec{u})$ with eight minima along the $\langle 111 \rangle$ directions. The depth of the potential well ΔF_m is ≈ 15 meV just above T_c. Since $k_B T_c \geq \Delta F_m$, each local mode component can overcome easily the free-energy barrier ΔF_m separating these eight minima, which explains the observed frequent oscillations.

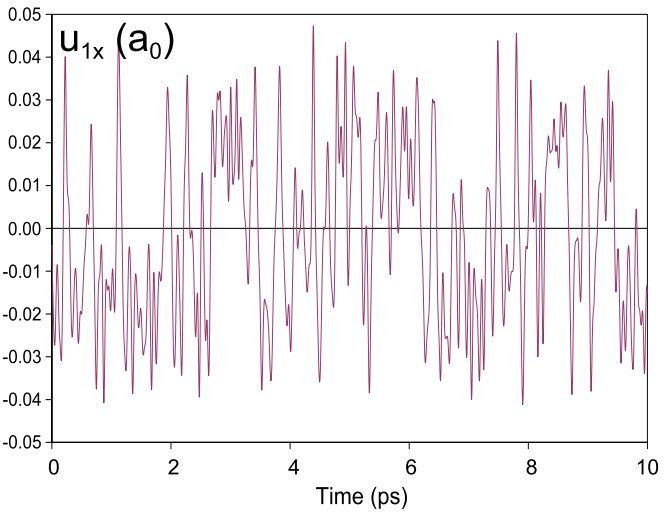

FIG. 7. (Color online) Example of time evolution (NVE ensemble) of the x component of a selected local mode at $T=314$ K (i.e., just above T_c). The local mode x component is in a_0 units (a_0 is the lattice constant).

D. Density of probability of the local mode components

We define $\Pi_\alpha(u_\alpha)$ as the density of probability of the α component of the local modes: in an equilibrated system with N unit cells (thus N local modes), at a given time t, the number of local modes having their α component between u_α and $u_\alpha + du_\alpha$ is $N\Pi_\alpha(u_\alpha)du_\alpha$.

In the paraelectric phase, it is obvious that the three functions Π_x, Π_y, and Π_z are the same. They can be calculated from the density of probability $\Pi(\vec{u})$ defined above,

$$\Pi_x(u_x) = \int_{-\infty}^{+\infty} du_y \int_{-\infty}^{+\infty} du_z \, \Pi(u_x, u_y, u_z),$$

$$\Pi_x(u_x) = \Pi_0 \int_{-\infty}^{+\infty} du_y \int_{-\infty}^{+\infty} du_z \, e^{-\Delta \tilde{F}(\vec{u})/k_B T}. \quad (23)$$

Interestingly, this quantity has been calculated in the pioneering work of Zhong *et al.*[9] with the same Hamiltonian. It presents two maxima above T_c, which decrease when the temperature increases until $\Pi_x(u_x)$ has only one maximum for $u_x=0$.

To validate our computation of the local free energy $\tilde{F}$, we calculate now from direct molecular-dynamics simulations the functions $\Pi_\alpha(u_\alpha)$ for six temperatures above T_c. These calculations are performed in the NVE ensemble and consist of 60 000 steps of equilibration followed by 100 000 steps for the calculation of $\Pi_\alpha(u_\alpha)$ (500 000 in the case of the two lowest temperatures). To calculate the densities of probability $\Pi_x(u_x)$, $\Pi_y(u_y)$, and $\Pi_z(u_z)$, we examine the values of u_x, u_y, and u_z for each dipole and each time step of the equilibrated trajectory (this gives 172.8×10^6 values and provides a very good statistics) and count how many local modes have their components u_α between values separated by $\Delta u_\alpha = 0.001 a_0$. The results are plotted on Fig. 8.

As expected, the profiles exhibit two pronounced maxima just above T_c. But this double maximum profile is lost between 400 and 500 K, thus much below the T_0 found from the previous computations of $\tilde{F}$ (between 500 and 700 K, the density of probability has two maxima along [111] from our computation of $\tilde{F}$).

This discrepancy is only apparent since the densities of probability of the local mode components are obtained through integration over two variables. Thus we use the analytical expression of $\tilde{F}(\vec{u})$ previously determined and perform numerically the integration of Eq. (23). The obtained profiles for the six temperatures of Fig. 8 are shown on Fig. 9 and are in good agreement with the direct calculations of Fig. 8. The agreement with The Monte Carlo calculations of Zhong *et al.* (Fig. 5 of Ref. 9) is also very good.

V. DISCUSSION

A. Local thermodynamic potential and averaged potential

We point out that the local thermodynamic potential $\tilde{F}(\vec{u})$ defined and computed above is not the same quantity as the

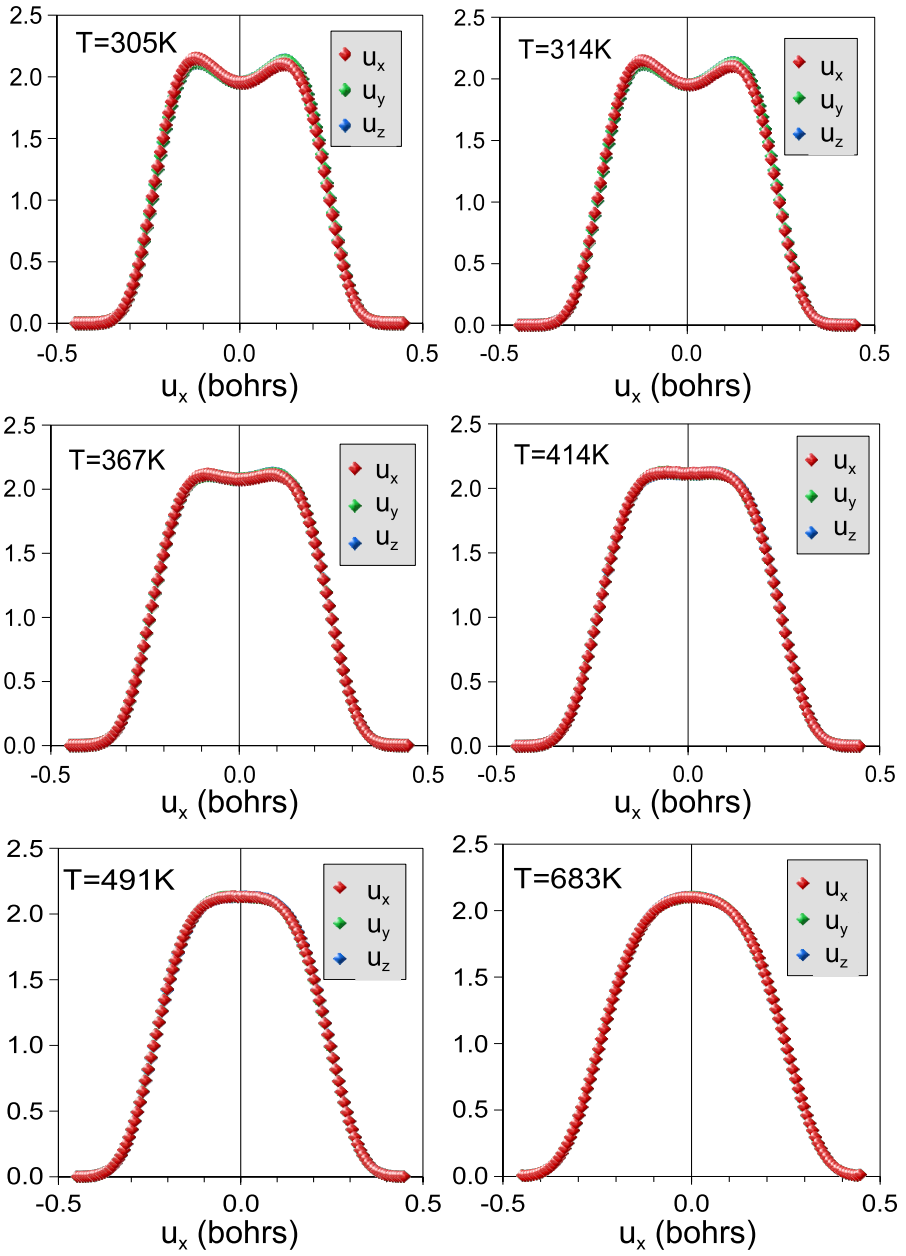

FIG. 8. (Color online) Density of probability of the local modes components $\Pi_x(u_x)$, $\Pi_y(u_y)$, and $\Pi_z(u_z)$ for six temperatures above T_c, obtained by direct counting over a long enough equilibrated MD trajectory. The densities of probability are in bohr^{-1}. u_x is in atomic units (bohrs).

averaged potential calculated by Marqués.[18] This author calculated the thermal average of the instantaneous *potential energy surface* seen by a given local mode. In our case, the computation of the thermodynamic potential at $\vec{u}$ requires only the configurations for which the selected local mode equals $\vec{u}$ (this is achieved by constrained dynamics).

In other words, among all the microscopic configurations forming an equilibrium trajectory, we retain only those for which $\vec{u}_1=\vec{u}$ to calculate the free energy at $\vec{u}$ whereas in the approach of Marqués, all the potential energy surfaces of the trajectory are taken into account to compute the average potential. Thus, this is not the same physical quantity. This explains the apparent discrepancy with the potential profile plotted along the [100] direction at $T=400$ K by this author (single minimum at $\vec{u}=\vec{0}$).

The numerical approach we have used (thermodynamic integration) could be replaced with equivalent methods (umbrella sampling, free-energy perturbation) that allow more practical implementation within Monte Carlo methods rather than molecular dynamics.

The local free energy defined in this work has to be distinguished from the Landau free energy. The Landau free energy can be also defined as an incomplete free energy (that can be computed also by thermodynamic integration[21]), but the restriction is over the microscopic states having a given polarization (long-range order parameter).[21,28] It contains information about the long-range polar order in the system, whereas the present free energy does not contain any information about long-range nor midrange polar order.

B. Off-center dipoles in barium titanate

Our results concerning the shape of the local free energy are in agreement with a set of recent experimental observa-

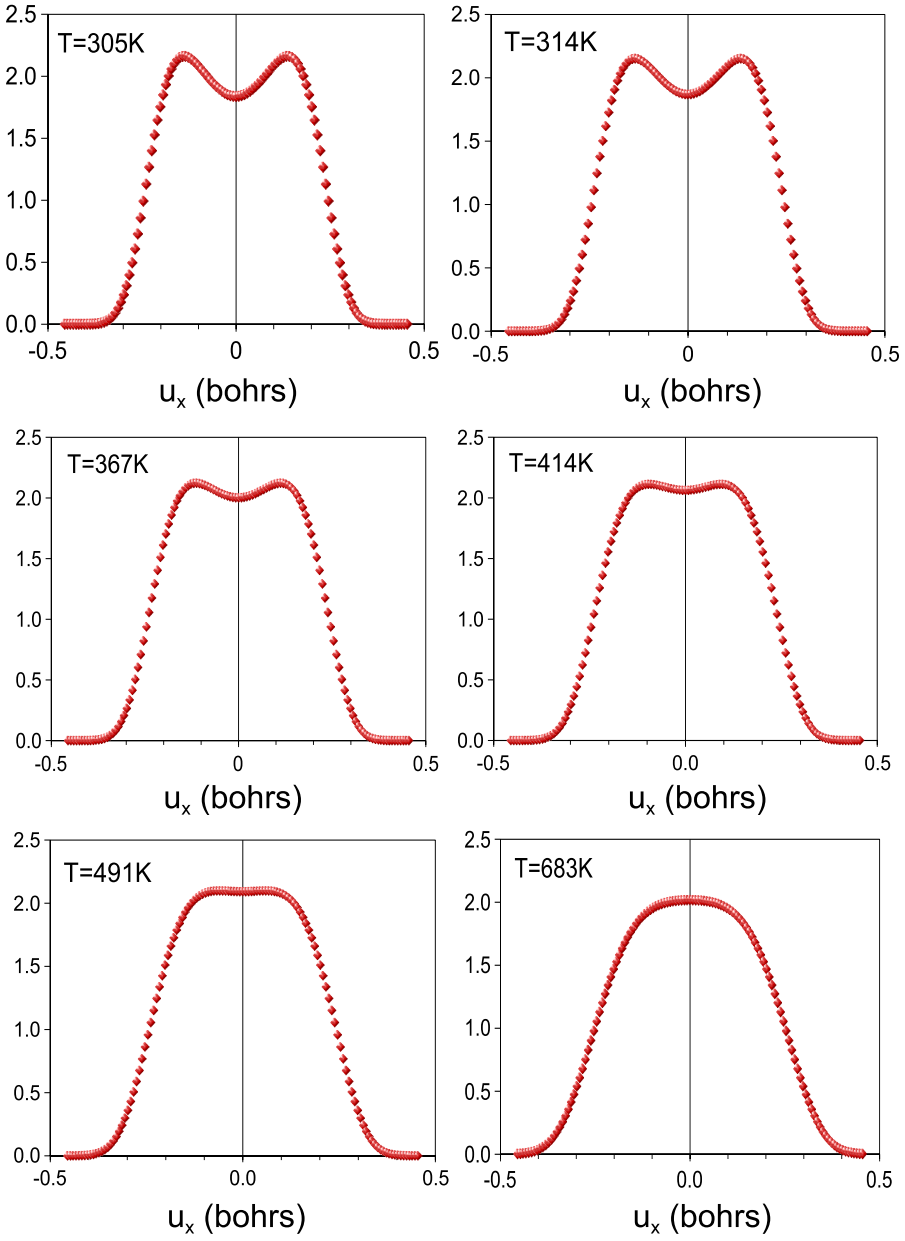

FIG. 9. (Color online) Density of probability of the local modes components $\Pi_x(u_x)$ according to Eq. (23) and the model for the free-energy coefficients a_1, a_{11}, and a_{12}. The densities of probability are in bohr^{-1}. u_x is in atomic units (bohrs).

tions, in particular the NMR experiments of Zalar *et al.*[31,32] that show the presence of off-center Ti in the paraelectric phase of barium titanate. It also confirms older Fe^{3+} electron-paramagnetic-resonance (EPR) experiments showing strong local anharmonicity in the displacements of Ti in the cubic phase of barium titanate.[8]

Thus in the paraelectric phase of barium titanate, the Ti ions (or more precisely the local modes that consist of local collective displacements in a given unit cell) are off center up to very high temperatures. Between T_c and $\approx T_c+400$ K, these local polar displacements minimize the free energy for nonzero values located along the ⟨111⟩ directions, which gives eight maxima of the density of probability in these sites. This gives support to the well-known pure order-disorder model of Comes *et al.*[33] and Chaves *et al.*[34] in which the Ti ions occupy eight sites located along the ⟨111⟩ directions.

The dynamics of the dipoles in the paraelectric phase of barium titanate has thus a strong order-disorder character. Anyway, the depth of the thermodynamic potential well ΔF_m just above T_c is only $\approx$15 meV, i.e., very close to $k_B T_c \approx 25$ meV. The limiting case of pure order-disorder systems for which $k_B T_c \ll \Delta F_m$ is thus not reached. It means that just above T_c, the local modes oscillate in the eight free-energy minima located along the ⟨111⟩ directions but do not stay for a long time in each of them: they jump very frequently from a minimum to another, as shown by the dynamics of Fig. 7. Moreover, the local modes evolve from a minimum to another by crossing (100) planes, involving therefore a free-energy barrier $\approx$5 meV (Fig. 5). The thermal energy at T_c is thus much larger than the thermodynamic potential barriers separating the local minima. By counting how many times the local mode component of Fig. 7 changes its sign in 10 ps, it is possible to estimate at $\approx$0.1–0.2 ps the order of magnitude of the mean time spent in one minimum of the free energy just above T_c.

This very short time, associated to the small free-energy barrier separating the eight minima (that can be overcome

easily), confirms the mixed displacive order-disorder character of the high-temperature phase of barium titanate. This short time is also at the root of the soft mode overdamping phenomena observed when the temperature decreases down to T_c.

It could be interesting, following the paper of Müller and Berlinger,[8] to calculate a parameter $o=\Delta F_m/k_B T_c$, in which ΔF_m is the depth of the local thermodynamic potential just above the Curie temperature. In the case of a purely order-disorder system, we have $o \to +\infty$, whereas for a displacive system, $o \to 0$. In practice, real systems lie of course in between, with a character more or less pronounced in favor of order-disorder or displacive. The approach presented in this work allows a numerical determination of this parameter that quantifies the degree of order-disorder in a ferroelectric. For barium titanate (and using the effective Hamiltonian of Zhong *et al.*[9]), this parameter is $o \approx 0.6$.

At high temperature ($T \to 700$ K), the free energy has finally its minimum at $\vec{u}=\vec{0}$. Anyway, it does not mean that the dynamics recovers a displacive character since the free energy is still strongly anharmonic at this temperature (the quadratic term crosses zero, leading to a very flat free-energy landscape).

C. Future extension to other phases and other systems

The concept of local thermodynamic potential can be extended easily to the ferroelectric phases of barium titanate (or any other ferroelectric). For instance, in the tetragonal phase, it is possible to perform the same constrained molecular-dynamics simulations by fixing a selected local mode $\vec{u}_1$ to a given value $\vec{u}$. The resulting landscape should exhibit a strong minimum when $\vec{u}$ is parallel to the polarization in the material, but it would be interesting to examine the possible existence of local minima below T_c. Indeed recent measurements and theoretical studies[35] suggest the existence of order-disorder phenomena even in the ferroelectric phase just below the phase transition. The same kind of processes has also been recently evidenced through electron paramagnetic resonance in the low-temperature rhombohedral phase of barium titanate.[36]

The extension seems more difficult in complex solids such as relaxors, in which the different sites are not equivalent. In that case, the local free energy should rather be computed directly from the density of probability if possible or by averaging the local potentials computed at several sites.

VI. CONCLUSION

In this work, a suitable definition has been proposed for the local potential seen by a local mode $\vec{u}$ in the paraelectric phase of a ferroelectric crystal, as the potential associated to the mean force felt by this local mode. We have shown that this potential of mean force is an incomplete free energy $\tilde{F}(\vec{u})$ and can be computed by constrained molecular dynamics coupled to the method of the thermodynamic integration. We have called it a *local* thermodynamic potential. It has been also shown that the density of probability of the local modes is directly related to this free-energy landscape through the simple relation $\Pi(\vec{u})=\Pi_0 e^{-[\tilde{F}(\vec{u})-\tilde{F}_0]/k_B T}$.

This local free-energy landscape, computed in the framework of the effective Hamiltonian of Zhong *et al.*,[9] exhibits for barium titanate eight minima along the $\langle 111 \rangle$ directions between T_c and $\approx T_c+400$ K. Above T_c+400 K, only one minimum is found for $\vec{u}=\vec{0}$. At T_c, the depth of the free-energy surface is ≈ 15 meV. This is approximately the order of magnitude of $k_B T_c$ and gives support, for barium titanate, to a ferroelectric-paraelectric phase transition with both displacive and order-disorder components. In the paraelectric phase of barium titanate, and in the framework of the effective Hamiltonian of Zhong *et al.*,[9] the local thermodynamic potential can be very well modeled as

$$\begin{aligned}\tilde{F}(\vec{u}) - \tilde{F}_0 &= \Delta\tilde{F}(\vec{u}) \\ &= a_1(u_x^2+u_y^2+u_z^2) + a_{11}(u_x^4+u_y^4+u_z^4) \\ &\quad + a_{12}(u_x^2u_y^2+u_x^2u_z^2+u_y^2u_z^2)\end{aligned}$$

with the coefficients and their temperature dependence in the range of 300–700 K given in Table I.

*gregory.geneste@ecp.fr

[1] W. P. Mason and B. T. Matthias, Phys. Rev. **74**, 1622 (1948).
[2] J. C. Slater, Phys. Rev. **78**, 748 (1950).
[3] E. T. Jaynes, Phys. Rev. **79**, 1008 (1950).
[4] W. Cochran, Adv. Phys. **9**, 387 (1960).
[5] W. Cochran, Phys. Status Solidi **30**, K157 (1968).
[6] J. Harada, J. D. Axe, and G. Shirane, Phys. Rev. B **4**, 155 (1971).
[7] P. A. Fleury and J. M. Worlock, Phys. Rev. **174**, 613 (1968).
[8] K. A. Muller and W. Berlinger, Phys. Rev. B **34**, 6130 (1986).
[9] W. Zhong, D. Vanderbilt, and K. M. Rabe, Phys. Rev. B **52**, 6301 (1995).
[10] M. Stachiotti, A. Dobry, R. Migoni, and A. Bussmann-Holder, Phys. Rev. B **47**, 2473 (1993).
[11] A. Bussmann-Holder and A. R. Bishop, Phys. Rev. B **56**, 5297 (1997).
[12] A. Bussmann-Holder, Physica B **263–264**, 408 (1999).
[13] Ph. Ghosez, Ph.D. thesis, Université Catholique de Louvain, 1997.
[14] W. Zhong, D. Vanderbilt, and K. M. Rabe, Phys. Rev. Lett. **73**, 1861 (1994).
[15] I. A. Kornev, L. Bellaiche, P.-E. Janolin, B. Dkhil, and E. Suard, Phys. Rev. Lett. **97**, 157601 (2006).
[16] I. A. Kornev, S. Lisenkov, R. Haumont, B. Dkhil, and L. Bellaiche, Phys. Rev. Lett. **99**, 227602 (2007).
[17] G. Geneste, E. Bousquet, and Ph. Ghosez, J. Comput. Theor. Nanosci. **5**, 517 (2008).
[18] M. I. Marqués, Phys. Rev. B **71**, 174116 (2005).

[19] D. Alfè and M. J. Gillan, J. Chem. Phys. **127**, 114709 (2007).
[20] G. Boisvert, N. Mousseau, and L. J. Lewis, Phys. Rev. B **58**, 12667 (1998).
[21] G. Geneste, Phys. Rev. B **79**, 064101 (2009).
[22] G. Geneste, arXiv:0901.3571 (unpublished).
[23] M. Parrinello and A. Rahman, Phys. Rev. Lett. **45**, 1196 (1980).
[24] S. Nosé, J. Chem. Phys. **81**, 511 (1984).
[25] S. Nosé, Mol. Phys. **57**, 187 (1986).
[26] W. G. Hoover, Phys. Rev. A **31**, 1695 (1985).
[27] T. Nishimatsu, U. V. Waghmare, Y. Kawazoe, and D. Vanderbilt, Phys. Rev. B **78**, 104104 (2008).
[28] J. Íñiguez, S. Ivantchev, J. M. Perez-Mato, and A. Garcia, Phys. Rev. B **63**, 144103 (2001).
[29] G. Geneste (unpublished).
[30] In the present case, the vanishing of this parameter does not correspond to any phase transition.
[31] B. Zalar, V. V. Laguta, and R. Blinc, Phys. Rev. Lett. **90**, 037601 (2003).
[32] B. Zalar, A. Lebar, J. Seliger, R. Blinc, V. V. Laguta, and M. Itoh, Phys. Rev. B **71**, 064107 (2005).
[33] R. Comes, M. Lambert, and A. Guinier, Solid State Commun. **6**, 715 (1968).
[34] A. S. Chaves, F. C. S. Barreto, R. A. Nogueira, and B. Zēks, Phys. Rev. B **13**, 207 (1976).
[35] J. Hlinka, T. Ostapchuk, D. Nuzhnyy, J. Petzelt, P. Kuzel, C. Kadlec, P. Vanek, I. Ponomareva, and L. Bellaiche, Phys. Rev. Lett. **101**, 167402 (2008).
[36] G. Volkel and K. A. Muller, Phys. Rev. B **76**, 094105 (2007).